



Contents lists available at ScienceDirect

Journal of Advanced Research

journal homepage: [www.elsevier.com/locate/jare](http://www.elsevier.com/locate/jare)

Original Manuscript

## Enhanced LRP8 expression induced by *Helicobacter pylori* drives gastric cancer progression by facilitating $\beta$ -Catenin nuclear translocation

Bin Liu<sup>a,b,1</sup>, Ihtisham Bukhari<sup>a,b,1</sup>, Fazhan Li<sup>a,b</sup>, Feifei Ren<sup>a</sup>, Xue Xia<sup>a</sup>, Baitong Hu<sup>a,b</sup>, Haipeng Liu<sup>c</sup>, Thomas F Meyer<sup>d,e</sup>, Barry J. Marshall<sup>f</sup>, Alfred Tay<sup>f</sup>, Yuming Fu<sup>g</sup>, Wanqing Wu<sup>g</sup>, Youcai Tang<sup>h</sup>, Yang Mi<sup>a,\*</sup>, Peng-Yuan Zheng<sup>a,\*</sup>

<sup>a</sup> Henan Key Laboratory for *Helicobacter pylori* and Digestive Tract Microecology, Marshall Medical Research Center, The Fifth Affiliated Hospital of Zhengzhou University, Zhengzhou 450052, Henan, China

<sup>b</sup> Academy of Medical Science, Zhengzhou University, Zhengzhou 450001, Henan, China

<sup>c</sup> Clinical and Translational Research Center, Shanghai Pulmonary Hospital, Tongji University School of Medicine, Shanghai 200433, China

<sup>d</sup> Max Planck Institute for Infection Biology, Department of Molecular Biology, 10117 Berlin, Germany

<sup>e</sup> Laboratory of Infection Oncology, Institute of Clinical Molecular Biology (IKMB), Christian-Albrechts University of Kiel, Kiel, Germany

<sup>f</sup> *Helicobacter Pylori* Research Laboratory, School of Biomedical Sciences, Marshall Centre for Infectious Disease Research and Training, University of Western Australia, Nedlands 6009, Australia

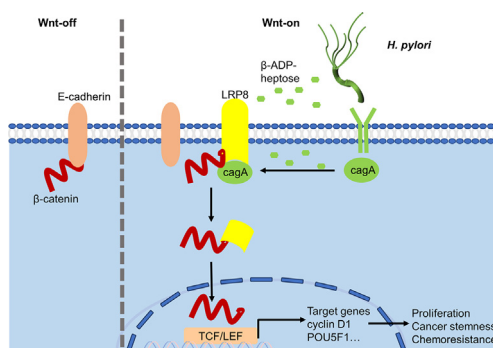
<sup>g</sup> Gastrointestinal Surgery, The Fifth Affiliated Hospital of Zhengzhou University, Zhengzhou 450052, Henan, China

<sup>h</sup> Department of Pediatrics, the Fifth Affiliated Hospital of Zhengzhou University, Zhengzhou, 450052, China

## HIGHLIGHTS

- *H. pylori* infection transcriptionally upregulated LRP8 expression in GC tissues, cell lines and organoids.
- LRP8 promotes stemness and proliferation of GC cells and organoids via enhancing  $\beta$ -catenin transcriptional activity.
- LRP8 serves as a molecular bridge, engaged with  $\beta$ -catenin to form the cagA/LRP8/ $\beta$ -catenin complex. This interaction disrupts the E-cadherin/ $\beta$ -catenin complex and facilitates the nuclear translocation of  $\beta$ -catenin.
- LRP8 contributes to chemoresistance in GC cells and organoids, specifically to 5-Fluorouracil treatment.

## GRAPHICAL ABSTRACT



## ARTICLE INFO

## Article history:

Received 1 February 2024

Revised 5 April 2024

Accepted 5 April 2024

Available online xxxx

## ABSTRACT

**Introduction:** *Helicobacter pylori* (*H. pylori*) infection has been associated with gastric carcinogenesis. However, the precise involvement of LRP8, the low-density lipoprotein receptor-related protein 8, in *H. pylori* pathogenesis and gastric cancer (GC) remains poorly understood.

**Objectives:** To investigate the potential role of LRP8 in *H. pylori* infection and gastric carcinogenesis.

**Abbreviations:** GC, gastric cancer; *H. pylori*, *Helicobacter pylori*; LRP8, low-density lipoprotein receptor-related protein 8; CSCs, cancer stem cells, hGO, human gastric organoid, hGCO, human gastric cancer organoid; RNAss, RNA stemness score; EV, empty vector; OV, overexpression vector; 5-FU, 5-Fluorouracil; IC50, median inhibitory concentration; MDR, multidrug resistance genes; TCGA, The Cancer Genome Atlas; GEO, Gene Expression Omnibus; ELISA, enzyme-linked immunosorbent assay; MOI, multiplicity of infection; RT-qPCR, real-time fluorescent quantitative polymerase chain reaction; IB, Immunoblotting; Co-IP, Co-Immunoprecipitation; IF, Immunofluorescence.

\* Corresponding authors at: The Fifth Affiliated Hospital of Zhengzhou University, Zhengzhou 450052, Henan, China.

E-mail addresses: [pyzheng@zzu.edu.cn](mailto:pyzheng@zzu.edu.cn) (P.-Y. Zheng), [yangmi198@zzu.edu.cn](mailto:yangmi198@zzu.edu.cn) (Y. Mi).

<sup>1</sup> These authors contributed equally to this work

<https://doi.org/10.1016/j.jare.2024.04.002>

2090-1232/© 2023 The Authors. Published by Elsevier B.V. on behalf of Cairo University.

This is an open access article under the CC BY-NC-ND license (<http://creativecommons.org/licenses/by-nc-nd/4.0/>).

Please cite this article as: B. Liu, I. Bukhari, F. Li et al., Enhanced LRP8 expression induced by *Helicobacter pylori* drives gastric cancer progression by facilitating  $\beta$ -Catenin nuclear translocation, Journal of Advanced Research, <https://doi.org/10.1016/j.jare.2024.04.002>

**Keywords:**

Gastric cancer  
LRP8  
*Helicobacter pylori*  
Wnt/ $\beta$ -catenin  
Organoids  
CagA

**Methods:** Three-dimensional human-derived gastric organoids (hGO) and gastric cancer organoids (hGCO) were synthesized from the tissues obtained from human donors. In this work, multi-omics combined with *in vivo* and *in vitro* studies were conducted to investigate the potential involvement of LRP8 in *H. pylori*-induced GC.

**Results:** We found that *H. pylori* infection significantly upregulated the expression of LRP8 in human GC tissues, cells, organoids, and mouse gastric mucous. In particular, LRP8 exhibited a distinct enrichment in cancer stem cells (CSC). Functionally, silencing of LRP8 affected the formation and proliferation of tumor spheroids, while increased expression of LRP8 was associated with increased proliferation and stemness of GC cells and organoids. Mechanistically, LRP8 promotes the binding of E-cadherin to  $\beta$ -catenin, thereby promoting nuclear translocation and transcriptional activity of  $\beta$ -catenin. Furthermore, LRP8 interacts with the cytotoxin-associated gene A (CagA) to form the CagA/LRP8/ $\beta$ -catenin complex. This complex further amplifies *H. pylori*-induced  $\beta$ -catenin nuclear translocation, leading to increased transcription of inflammatory factors and CSC markers. Clinical analysis demonstrated that abnormal overexpression of LRP8 is correlated with a poor prognosis and resistance to 5-Fluorouracil in patients with GC.

**Conclusion:** Our findings provide valuable information on the molecular intricacies of *H. pylori*-induced gastric carcinogenesis, offering potential therapeutic targets and prognostic markers for GC.

© 2023 The Authors. Published by Elsevier B.V. on behalf of Cairo University. This is an open access article under the CC BY-NC-ND license (<http://creativecommons.org/licenses/by-nc-nd/4.0/>).

**Introduction**

Gastric cancer (GC) ranks third among global cancer-related fatalities [1], in which *Helicobacter pylori* (*H. pylori*) is potentially responsible for around half of annual cases and fatalities, particularly in China [2]. *H. pylori* initiates a cascade of pathological processes, including Wnt/ $\beta$ -catenin pathway activation and GC stem cell proliferation [3].

The canonical Wnt/ $\beta$ -catenin pathway, initiated by Wnt ligands, triggers nuclear translocation of  $\beta$ -catenin and transcribes target genes [4,5]. The pathophysiology of *H. pylori* infection is intricately linked to sophisticated bacterial virulence mechanisms [6]. Among these, the cytotoxin-associated gene A (CagA), a well-documented virulence factor significantly activates the Wnt/ $\beta$ -catenin pathway, leading to the induction of inflammation [7,8]. Additionally, the recently identified virulence factor,  $\beta$ -ADP-heptose [9], has been shown to possess potent capabilities in triggering inflammatory responses [9,10]. This promotes the differentiation and proliferation of cancer stem cells (CSCs), leading to GC progression [11,12]. However, a comprehensive understanding of the intricate regulatory mechanisms underlying the virulence factor of *H. pylori* and the nuclear translocation of  $\beta$ -catenin in GC is not very well defined.

LRP8 is initially involved in physiological cell differentiation and lipid transport [13–15]. Recent evidence has highlighted its involvement in proliferation, migration, stemness, and chemosensitivity in various types of cancer [16–19]. However, the precise role of LRP8 in GC remains largely unknown. In the current study, we employed integrative methods to reveal the role of LRP8 in the regulation of the Wnt/ $\beta$ -catenin pathway independent of Wnt ligands. Furthermore, we investigated its bridge function in mediating the effects of *H. pylori* virulence factors (CagA and  $\beta$ -ADP-heptose) on stemness and inflammatory response. Our findings shed light on the functional significance of LRP8 in *H. pylori*-induced GC and offer potential therapeutic strategies for its treatment.

**Methods and materials***Cell lines and strains*

The human gastric epithelial cell line GES-1 and GC cell lines (SGC7901, MGC803, AGS, NCI-N87) were obtained from the Chinese National Collection of Authenticated Cell Cultures and maintained in RPMI1640 medium (Gibco, Grand Island, USA)

supplemented with 10 % Fetal Bovine Serum (Biological Industries, Kibbutz Beit Haemek, Israel) and 1 % penicillin/streptomycin (Gibco). The human embryonic kidney 293 cell line: HEK293T, also from the same supplier, was cultured in DEME medium (Gibco). All cell lines were authenticated by short tandem repeats (STR) analysis and cultured in mycoplasma-free conditions at 37 °C under a humidified atmosphere.

*H. pylori* strains (P12, GFP-P12, and CagA-deficient,  $\Delta$ CagA), Wnt3a, and Rspodin cells were generously gifted by Prof. Thomas [20]. The mouse-adapted *H. pylori* SS1 strain was a kind gift from Prof. Marshall [21,22]. *H. pylori* was cultured on Columbia Agar Base plates under microaerophilic conditions at 37 °C, with passages every three days.

*Patients*

A total of 55 stomach tissue samples were collected (September 2021 to December 2022) from patients who underwent total or partial gastric resection at the Fifth Affiliated Hospital of Zhengzhou University. Paired adjacent tissues more than 10 cm away from the tumor were collected. The *H. pylori*-infection status of the patients was determined by C13-urea respiratory test and retrospective immunohistochemistry.

*Animals*

Male C57BL/6Cnc mice were purchased from Vital River Laboratory (Beijing, China). 5–6 weeks-old mice were exposed to N-Methyl-N-nitrosourea (MNU, Sigma-Aldrich, St. Louis, MO, USA) at a concentration of 150 ppm for 5 weeks. The *H. pylori* SS1 suspension with  $2 \times 10^8$  CFU was administered orally to mice 7 times. Control mice were treated with an equal volume of Brain-Heart Infusion Broth (BHI, OXOID, MA, USA) solution. All mice were sacrificed after 18 weeks, and stomach tissues were meticulously extracted for further analysis.

*Ethics statement*

All studies involving human biospecies comply with the guidelines and ethical standards of the Helsinki Declaration of 1964 and the ARRIVE reporting guidelines. Also, all procedures and experiments used in this study were approved by the Ethics Committee of the Fifth Affiliated Hospital of Zhengzhou University (License No: KY2020029 for the human experiments and

KY2021028 for the animal experiments) and informed written consent was obtained from all participants.

### Immunohistochemistry

Immunohistochemical staining was performed according to our previously published protocol [23]. Briefly, the anti-LRP8 primary antibody (Supplementary Table 2) biotinylated secondary antibody, and horseradish enzyme-labelled streptavidin were used to detect LRP8. Diaminobenzidine and hematoxylin were then stained. The images were scored using the German semi-quantitative scoring method.

### Human gastric cancer patients-derived organoids(hGCO)

For the culture of hGOs and hGCOs, we adhered to the protocol previously published [20]. Simply, tumor tissues and adjacent tissues were digested into single cells and resuspended in Matrigel (Becton, Dickinson, NJ, USA). The organoids were cultured in organoid medium: Advanced DMEM/F12 Medium (Gibco) supplemented with 50 % Wnt3a and 25 % R-spondin conditional medium, 100 ng/mL human Noggin (Peprotech, NJ, USA), 1 % B27 (Invitrogen, CA, USA), 1 % N-2 (Invitrogen), 4 mM Nicotinamide (Sigma-Aldrich), 200 ng/mL human fibroblast growth factor-10 (FGF-10, Peprotech), 50 ng/mL epidermal growth factor (EGF, Invitrogen), 1 mM N-Acetyl-L-cysteine (Sigma-Aldrich), 1 nM Gastrin (Tocris, MN, USA), 0.5  $\mu$ M A83-01(Tocris), 10  $\mu$ M Y-27632 (Sigma-Aldrich).

### Small interfering RNA(siRNA)

si-RNA-LRP8 or si-NC (Jima, Shanghai, China) were transfected with jetPRIME<sup>®</sup> reagent (Polyplus, Strasbourg, France) according to the manufacturer's instructions. After 48 h of incubation, the cells were collected for subsequent experiments.

### Genes overexpression

To generate organoids and GC cells with ectopic overexpression of LRP8, we inserted the genomic sequence of human LRP8 into the pCDH-CMV-MCS-EF1-Puro vector (youbio, China, Changsha). To harvest viral particles, 293 T cells were transfected with 2  $\mu$ g plasmid (psPAX2/PMD2.G/pCDH-EV or pCDH-LRP8-OV in a 1:1:1 M ratio) using jetPRIME<sup>®</sup>, the supernatant was collected after 48 h. Next, 8  $\mu$ g/mL of polybrene (Solarbio, Beijing, China) was combined with individual cells and centrifuged at 600 g for 90 min. Following three days, the medium was supplemented with 6 $\mu$ g/mL puromycin for SGC7901 cells and 1 $\mu$ g/mL for organoids, the cells and organoids that stably expressed LRP8 were obtained after 14 days.

For the exogenous expression of CagA, the hemagglutinin (HA)-tagged CagA was inserted into the pcDNA3.1-HA plasmid and transiently transfected to cells and 18 h later cells were collected for analysis.

### Stem cell sphere-forming assay

Approximately 2000 cells were seeded in 6-well ultra-low adhesion plates (Corning, USA) with 2 mL stem cell medium: RPMI-1640 supplemented with 20 ng/mL EGF (PeproTech), 20 ng/mL FGF (PeproTech) and 2 % B27(Invitrogen), 0.4 % bovine serum albumin (BSA, Sigma-Aldrich) and 5  $\mu$ g/mL insulin (Wan-Bang, Beijing, China). The spheres were imaged using phase-contrast microscopy after 7 days and the number of spheres over 100  $\mu$ m in diameter was counted [24].

### H. Pylori infection

*H. pylori* grown on agar plates for two days were resuspended in liquid medium (89 % BHI + 10 % FBS + 1 % antibiotics, Solarbio, China) and incubated for 24 h, *H.pylori* was collected by centrifuging at 4500 rpm for 8 min, then incubated with cells at a multiplicity of infection (MOI = 100) and 12 h later cells were used for protein or RNA extraction.

For infecting organoid with *H.pylori*, organoids were cultured in Wnt/Rspo-free medium for 4 days to induce differentiation, individual organoids were collected using cell recovery solution (Corning) and then mixed with GFP-*H. pylori* before suspending in matrigel. Following a 4-day co-culture period, RNA was extracted for further experiments.

### Real-time fluorescent quantitative PCR (RT-qPCR)

Total RNA was extracted by Trizol (Thermofish), and cDNA was obtained according to the instructions of the HiScript II 1st Strand cDNA Synthesis Kit (Vazamy, Nanjing, China). The qPCR mix was prepared as SYBR Green PCR Master Mix (Vazamy). The relative expression was calculated using the  $2^{-\Delta\Delta C_t}$  method [25]. All primer sequences are shown in Supplementary Table 3.

### Enzyme-linked immunosorbent assay(ELISA)

The ELISA experiments were performed by following the manufacturer's protocol (Boster, Wuhan, China). Briefly, cell culture supernatants were transferred to 96-well plates pre-coated with interleukin-8 (IL-8) antibodies, after incubated with secondary antibody and color development solution, the optical density at 450 nm (OD450nm) was measured using a multifunctional enzyme marker and the concentration of IL-8 was determined by referencing a standard curve.

### Nuclear protein extraction

The nuclear and cytoplasmic proteins were separated from the cells after fractionating cells using NE-PER<sup>™</sup> Nuclear and Cytoplasmic extraction kit by the manufacturer's instructions (Thermo Fisher). Briefly, cells were lysed with the cytoplasmic protein extraction reagents CER I and CER II, and the supernatants were used for cytoplasmic protein precipitation. The sediments were resuspended with ice-cold NER reagent for nuclear protein extraction. The isolated proteins were stored at  $-80^{\circ}\text{C}$  until subsequent use.

### Immunoblotting (IB)

The SDS-PAGE gels were prepared according to the kit instructions (Yase Biologicals, Beijing, China). Primary antibody (Supplementary Table 4) was added and incubated overnight at  $4^{\circ}\text{C}$ . The next day the secondary antibody was incubated at room temperature for 1 h. The blots were captured on camera using a Bio-RAD exposure meter.

### Co-immunoprecipitation (Co-IP)

The protein-protein interactions were identified by Co-IP assays. To summarize, protein A/G Magnetic Beads (MedChemExpress, USA) and specific antibodies (Supplementary Table 2) were mixed in 1.5 mL Eppendorf tubes and placed on the horizontal rotator at  $4^{\circ}\text{C}$  for 4 h to generate antibody-magnetic bead complexes, and mouse or rabbit IgG antibodies were used as negative control. Proteins were lysed using mild lysis buffer for 30 min, then incubated with antibody-magnetic beads complex overnight at  $4^{\circ}\text{C}$ .

to create a protein-antibody-magnetic beads complex; then washed and used for immunoblotting.

#### Immunofluorescence (IF)

Cells were fixed in 2 % paraformaldehyde and incubated with 150  $\mu$ L of primary antibody and secondary antibody (Supplementary Table 2) for 1 h at room temperature, DAPI solution was used to stain the nuclei. The target proteins were imaged using a Confocal Laser Scanning Microscope (Carl Zeiss 880, Oberkochen, Germany), and Pearson's colocalization and overlap coefficients were generated using the Image J software (version: 1.8.0.112) as described previously [26,27].

#### Cytotoxicity assay

For the 5-Fluorouracil (Solarbio) sensitivity assay, cells were incubated with medium containing different concentrations of 5-FU (0  $\mu$ g/mL-500  $\mu$ g/mL) for 48 h. For the proliferation curve assay, cells were incubated with 5-FU (10  $\mu$ g/mL and 50  $\mu$ g/mL) for 0, 24, 48 and 72 h. Then medium containing 10 % Cell Counting Kit-8 (Dojindo, Japan) was replaced, and the OD450 value was measured after incubation for 2 h in the dark. The activity of cells was evaluated as  $(OD450_{\text{experimental group}} - OD450_{\text{control group}}) / (OD450_{\text{experimental group}} + OD450_{\text{control group}}) \times 100 \%$ , and the IC50 and proliferation curves were calculated in GraphPad 9.0 software.

#### Cell apoptosis

Cells were treated with 5-FU (0, 10 and 50  $\mu$ g/mL) for 48 h. The Annexin V-FITC staining was performed according to the manufacturer's instructions (Keygentec, Jiangsu, China) and apoptotic cells were detected using flow cytometry (BD, Accuri™ C6). All the experiments were repeated independently at least thrice.

#### Statistics

All quantitative data were statistically analyzed using the paired Two-tailed Student's *t*-test or Satterthwaite test using SPSS 25.0 (SPSS, Chicago, IL, USA) and GraphPad 9.0 software (Boston, MA, USA), and immunohistochemistry scores were analyzed using Wilcoxon matched-pairs signed-ranks sum test. Survival analysis was performed using the log-rank test at the K-M plotter database. *p*-value < 0.05 was considered significant.

## Results

#### LRP8 overexpression in GC tissues, cell lines, and organoids

The analysis of TCGA data sets revealed a significant upregulation of LRP8 in GC tissues (Fig. 1A). The subgroup analysis showed that patients older than 65 years having intestinal type of GC according to the Lauren classification specifically have high

expression of LRP8 (Fig. 1B, C). Furthermore, we verified this by examining 55 paired samples of GC and adjacent non-cancer tissues; a significant increase in both mRNA and protein levels of LRP8 was observed in GC tissues (Fig. 1D-F). Additionally, LRP8 expression levels were significantly higher in three GC cell lines (AGS, MGC803, and NCI-N87) compared to the normal cell line GES-1 (Fig. 1G). Furthermore, a significant positive correlation ( $R^2 = 0.4007$ ,  $P < 0.05$ ) was identified between LRP8 expression and the CSC marker POU5F1 in GC tissues (Fig. 1H).

The role of LRP8 was further explored through *in vitro* cultivation of normal and GC organoids, which accurately reflect the characteristics of their tissue of origin. We detected a significant upregulation of the cancer marker HER2 in cancer organoids (Fig. S1), while hGCO exhibited considerably increased levels of LRP8 and POU5F1 expression as compared with hGO (Fig. 1J, K). These findings collectively underscore the significant elevation of LRP8 expression in human GC samples, suggesting its crucial role in the pathology of GC.

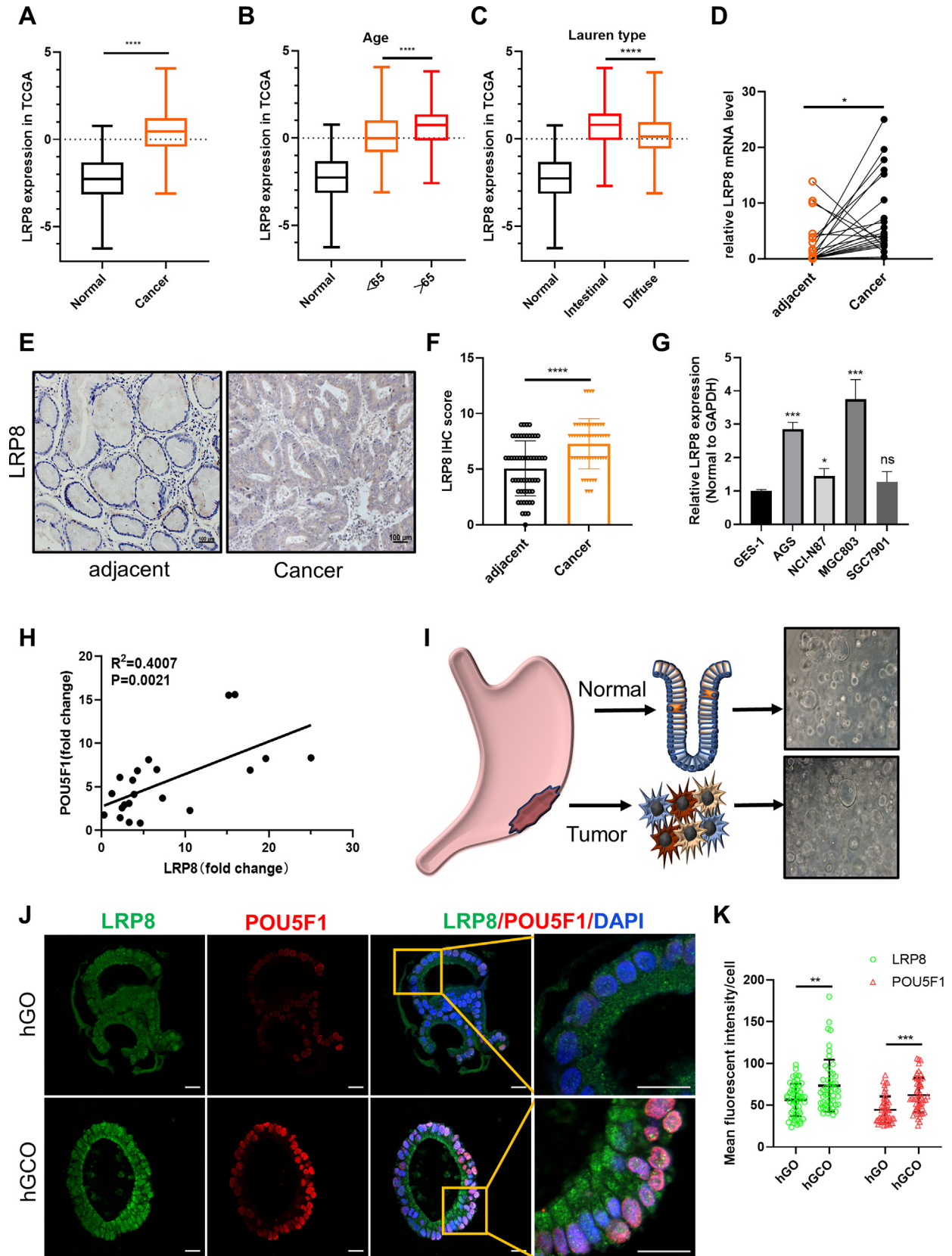
#### H. Pylori infection transcriptionally upregulated LRP8 expression

Analysis of two GEO datasets (GSE60662 and GSE60427) revealed an increased expression of LRP8 in *H. pylori*-positive gastric mucosa (Fig. 2A, B), we also detected high staining pattern of LRP8 in 55 GC tissue compared with adjacent tissue (Fig. 2C, D). Additionally, infection assays using *H. pylori* strains expressing green fluorescent protein (*GFP-Hp*) indicated scattered GFP foci in hGCO (Fig. 2E) and an increased expression of the inflammatory factor IL-8 (Fig. 2F). In particular, LRP8 expression was increased in *H. pylori*-infected organoids (Fig. 2F), and same pattern was observed in GC cell lines SGC7901 and MGC803 exposed to *H. pylori* (Fig. 2G).

To confirm these findings *in vivo*, 20 male C57BL/6cnc mice were infected with the *H. pylori* SS1 strain. These mice developed chronic atrophic gastritis (CAG), characterized by infiltration of polymorphonuclear neutrophils, a reduction in the original gastric glands, and dysplasia (Dys), marked by nuclear enlargement and an increased nucleus-to-cytoplasmic ratio. Immunohistochemical analysis confirmed *H. pylori* colonization on the mucosal surface and within the glandular lumen. Importantly, a significant upregulation of LRP8 expression was observed in tissues affected by CAG and Dys (Fig. 2H, I). These results highlight the role of *H. pylori* infection in modulating LRP8 expression.

Furthermore, we aimed to pinpoint the specific *H. pylori* virulence factors influencing LRP8 expression. Thus, we exposed SGC7901 cells with *H. pylori* P12 strains (both with and without the CagA) for 18 h, and detected overexpression of LRP8 in all cells with both strains (Fig. S2A). Additionally, we exogenously introduced HA-CagA into cells which did not alter LRP8 levels (Fig. S2A), suggesting an involvement of different *H. pylori* virulence factors in LRP8 regulation. Therefore, we then tested the  $\beta$ -ADP-heptose, derived from *H. pylori* was responsible for LRP8 upregulation in hGO (Fig. S2B, C) and SGC7901 cells

**Fig. 1. Overexpression of LRP8 in GC tissues, cell lines and organoids** A-C. LRP8 expression was analyzed in gastric cancer tissues and normal mucosa from the TCGA database (A). Differential expression of LRP8 was observed in gastric cancer patients of different age groups (B) as well as in different Lauren's staging (stomach and intestinal-type gastric cancer) (C). D. LRP8 mRNA expression was identified in 20 cases of cancer and adjacent tissues of gastric cancer patients by RT-qPCR. E. Representative immunohistochemical staining of LRP8 protein was performed in cancer and adjacent tissues, with a scale bar of 100  $\mu$ m. F. Immunohistochemistry scores were calculated for 55 cases of paired gastric cancer and adjacent tissues. G. Total RNA was extracted from GES-1 cells and 4 gastric cancer cells and the relative expression of LRP8 was determined in three independent experiments. H. Pearson correlation coefficient of LRP8 and POU5F1 expression in 20 gastric cancer samples. I. A schematic diagram for the culture of human patient-derived gastric (hGO) and gastric cancer organoids (hGCO). J. Immunofluorescence staining of LRP8 protein (green) and POU5F1 (red) were performed in hGO and hGCO, with DAPI (blue) indicating nuclei, scale bar: 20  $\mu$ m. K. The mean fluorescence intensities of LRP8 and POU5F1 are shown in the scatter plot ( $n = 50$  cells). (\*:  $p < 0.05$ , \*\*:  $p < 0.01$ , \*\*\*:  $p < 0.001$ , \*\*\*\*:  $p < 0.0001$ ). (For interpretation of the references to color in this figure legend, the reader is referred to the web version of this article.)



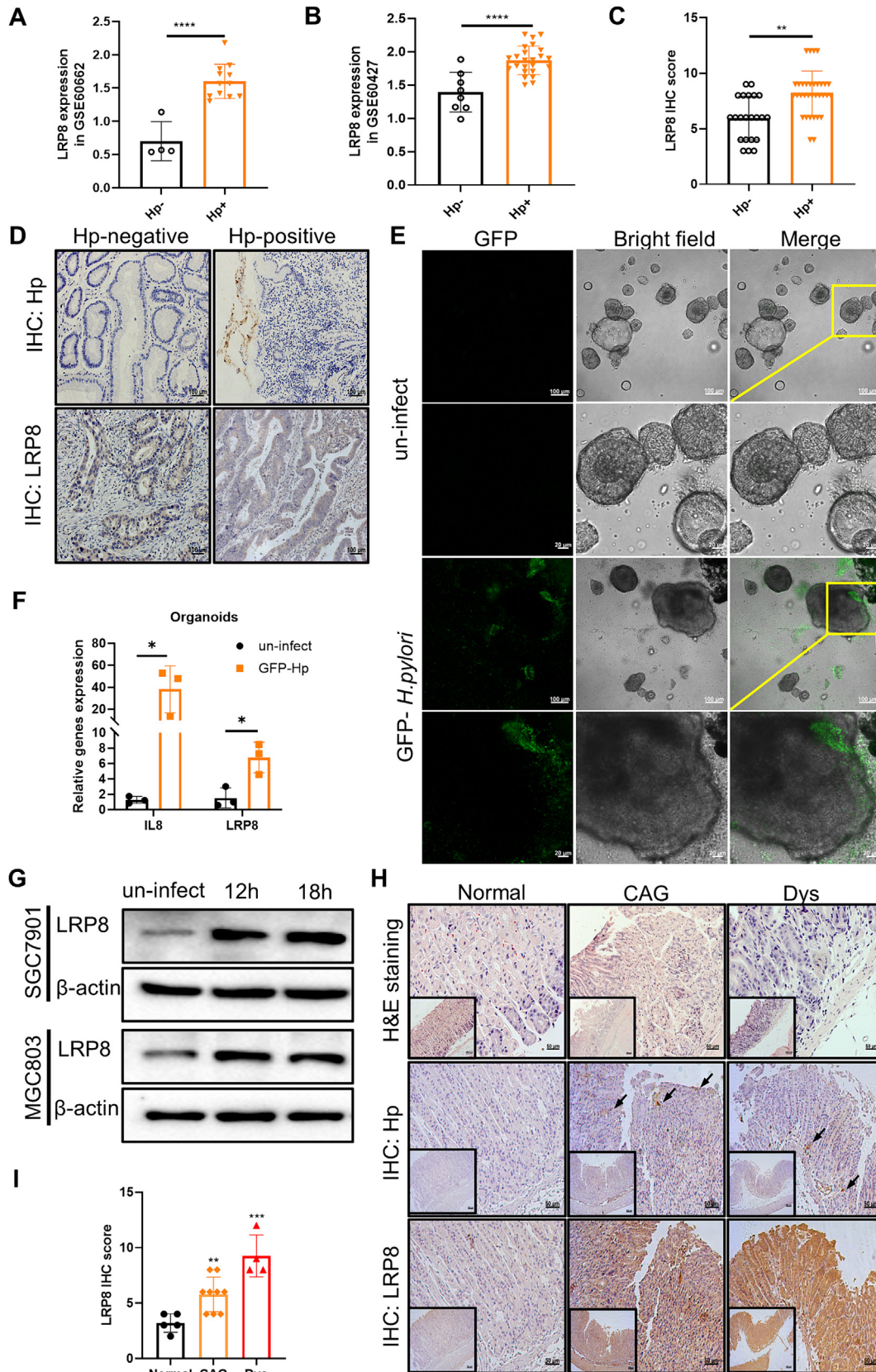


**Fig. 2. *H. pylori* infection transcriptionally upregulated LRP8 expression** A-B. Expression data of *LRP8* in *H. pylori*-infected gastric mucosa from GSE60662 and GSE60427 databanks. C. Immunohistochemical scoring of *LRP8* in 33 *H. pylori*-positive and 22 negative GC tissues. D. Representative immunohistochemical staining of *LRP8* protein and *H. pylori*. E. Microscopic imaging of gastric cancer organoids infected with GFP-*H. pylori* for 4 days, displaying *H. pylori* adhesion to the organoids. F. Expression of *LRP8* and inflammatory factor *IL8* in *H. pylori*-infected organoids detected using RT-qPCR. G. Western blot analysis of *LRP8* protein expression in uninfected MGC803 and SGC7901 cells and cells infected with *H. pylori* P12 strain for 12 and 18 h. H. Representative H&E staining and immunohistochemical staining images of *LRP8* and *H. pylori* (black arrow) in the gastric mucosa of mice (CAG: chronic atrophic gastritis; Dys: dysplasia). I. Immunohistochemical scoring of *LRP8* in mice. (\*:  $p < 0.05$ , \*\*:  $p < 0.01$ , \*\*\*:  $p < 0.001$ , \*\*\*\*:  $p < 0.0001$ ).

(Fig. S2D). These results unequivocally demonstrate a pivotal role of  $\beta$ -ADP-heptose in LRP8 regulation in transcription, thereby elucidating a novel aspect of the pathogenic mechanisms of *H. pylori*.

#### *LRP8 promotes stemness of GC cells and organoids*

Single-cell sequencing of the GSE134520 dataset demonstrated that LRP8 is predominantly expressed in malignant cells, with minimal presence in immune cells (Fig. S3A, B). This pattern was confirmed by analyzing the GSE112302 dataset, which showed LRP8 enrichment in both CSCs and malignant cells (Fig. S3C, D). Additionally, a positive correlation between LRP8 expression and the cancer RNA stemness score (RNAss) in GC tissues highlighted the oncogenic role of LRP8. (Fig. S3E). KEGG pathway analysis further implicated LRP8 is involved in the cell cycle and Wnt/ $\beta$ -catenin signaling (Fig. S3F).

To assess LRP8's functional impact, we silenced its expression in the MGC803 cells using specifically designed siRNAs (Fig. 3A, B), and ectopically overexpressed it in SGC7901 cells (Fig. 3C, D). Interestingly, we found that LRP8 knockdown significantly decreased sphere formation efficiency of the cells but we partially restored by supplementing stem cell medium with 20 % Wnt3a medium (Fig. 3E, F). In contrast, LRP8 overexpression increased sphere formation and induced large spheres in SGC7901 cells (Fig. 3G, H). The spheroids analysis found that the elimination of LRP8 significantly reduced the mRNA levels of key stemness markers (*POU5F1*, *ALDH1A1*, *CD15*, *CD44*) in MGC803 cells, while overexpression in SGC7901 cells significantly increased these markers.

Furthermore, LRP8 was overexpressed in hGCO using lentiviral system, which was confirmed by immunofluorescence and western blot analysis (Fig. 3K-M). This overexpression led to increased levels of *POU5F1*, *CD44*, *ALDH1A1* and *CD15* (Fig. 3K, M), highlighting LRP8's significant role in maintaining stemness of GC cells.

#### *LRP8 facilitates the activation of the Wnt/ $\beta$ -catenin pathway by promoting nuclear translocation of $\beta$ -catenin*

Our investigation of LRP8's involvement in the Wnt/ $\beta$ -catenin pathway revealed that silencing LRP8 in MGC803 cells did not affect  $\beta$ -catenin levels, yet significantly downregulated proteins essential for cellular proliferation, such as cyclin D1 and c-myc (Fig. 4A). In contrast, overexpression of LRP8 resulted in a significant upregulation of these proteins (Fig. 4B). To understand how LRP8 activates downstream signaling without altering  $\beta$ -catenin levels, we utilized the STRING database to predict interactions between LRP8 and key Wnt/ $\beta$ -catenin pathway proteins, which suggested a direct interaction between LRP8 and the  $\beta$ -catenin protein (encoded by *CTNNB1*), and a potential competitive interactions involving LRP8 and E-cadherin (encoded by *CDH1*) (Fig. 4C). Our immunofluorescence assay indicated LRP8 and  $\beta$ -catenin colocalization in SGC7901 cells (Fig. 4D-F); and Co-IP experiments further confirmed the mutual interaction between LRP8 and  $\beta$ -catenin. Thus we hypothesized that LRP8 facilitate the release of  $\beta$ -catenin from the  $\beta$ -catenin/E-cadherin complex, a crucial step in Wnt pathway activation.

Further investigation on the  $\beta$ -catenin/E-cadherin complex revealed that LRP8 overexpression led to a significant reduction in this complex's formation, suggesting LRP8 competes with E-cadherin for  $\beta$ -catenin binding (Fig. 4H). Subsequent cell fractionation showed a significant increase in nuclear  $\beta$ -catenin levels in cells with ectopic overexpression of LRP8 (Fig. 4I), reinforcing the notion that LRP8 promotes nuclear translocation of  $\beta$ -catenin and thereby activating the transcription of Wnt/ $\beta$ -catenin target genes. These findings suggest that LRP8 disrupts the  $\beta$ -catenin/E-cadherin complex through competitively binding to  $\beta$ -catenin, promoting

$\beta$ -catenin nuclear translocation and activating the Wnt/ $\beta$ -catenin pathway.

#### *H. Pylori infection induced $\beta$ -catenin transcriptional activity in a LRP8-dependent manner*

Investigating the role of LRP8 in *H. pylori* infection, we explored its impact on the nuclear translocation of  $\beta$ -catenin induced by the virulence factor CagA. We observed that *H. pylori* infection elevated nuclear  $\beta$ -catenin levels at 18 h post *H. pylori* –infection, an effect further enhanced in the cells overexpressing LRP8 (Fig. 5A-B), as demonstrated by cell fractionation analysis (Fig. 5C, D). We further verified the interaction between LRP8 and CagA by co-IP analysis, this interaction leads to the formation of a CagA/LRP8/ $\beta$ -catenin complex (Fig. 5E), thereby LRP8 promotes the association between CagA and  $\beta$ -catenin. Furthermore, we found that upon *H. pylori* infection a significant reduction in the  $\beta$ -catenin/E-cadherin complex formation was detected in LRP8-overexpressed cells (Fig. 5F), highlighting the key role of LRP8 in disrupting this complex. This disruption facilitates the release of  $\beta$ -catenin into the cytoplasm and its subsequent nuclear translocation. Suggesting a potential modulation of Wnt/ $\beta$ -catenin signaling in the context of *H. pylori* infection.

In addition, the modulation of LRP8 expression had a significant impact on inflammatory response and the activity of the Wnt/ $\beta$ -catenin pathway induced by *H. pylori*. LRP8 knockdown significantly inhibited *H.pylori*-induced IL-8 (Fig. 5G) and decreased expression of cyclin D1 and c-myc (Fig. 5H). On the contrary, LRP8 overexpression had an opposite effect (Fig. 5H). Furthermore, we observed an increase in the transcription of *CCND1* and *MYC* in response to  $\beta$ -ADP-heptose treatment (Fig. S2D) in SGC7901 cells. These findings highlight a complex regulatory network involving LRP8, *H. pylori* virulence factors, and the Wnt/ $\beta$ -catenin signaling pathway in GC.

#### *LRP8 promotes the proliferation and reduces the drug sensitivity of GC cells and organoids to 5-FU*

Cellular proliferation was evaluated through colony formation and transwell assays; LRP8 knockdown revealed a decreased number of colonies in MGC803 cells (Fig S4 A, B) and cellular migration (Fig. S4 E, F). Conversely, LRP8 overexpression significantly increased the number of colonies (Fig. S4C, D) and migration of SGC7901 cells (Fig. S4G, H). Notably, Wnt3a supplementation partially restored cellular viability and migration in LRP8-depleted cells (Fig. S3A, E). These findings underscore the importance of LRP8 in GC cellular proliferation, potentially linked to the Wnt/ $\beta$ -catenin pathway.

Drug resistance, particularly in GC, is a significant barrier to effective treatment and is often associated with a poor prognosis due to dysregulated oncogenes [28]. We also focused on LRP8's role in influencing chemosensitivity to 5-Fluorouracil (5-FU), a cornerstone in GC therapy. We found that LRP8-OV SGC7901 cells displayed increased resistance, with higher IC50 (27.64  $\mu$ g/mL) compared to it in LRP8-EV cells (11.75  $\mu$ g/mL) (Fig. 6A). This was further illustrated by proliferation assays, in which LRP8-OV cells showed higher growth rate in the absence of 5-FU and maintained higher resistance at lower drug concentrations (10  $\mu$ g/mL) (Fig. 6B). Flow cytometry analysis indicated that LRP8 overexpression reduced apoptosis rate in cells treated with 5-FU (Fig. 6C, D), aligning with the upregulation of multi-drug resistance (MDR) genes (Fig. 6E). This suggests that LRP8 may contribute to a multi-faceted mechanism of drug resistance, including alterations in cell survival pathways and efflux pump expression.

Leveraging the organoid model, imitating the complexity of tumor heterogeneity and drug responses more accurately than

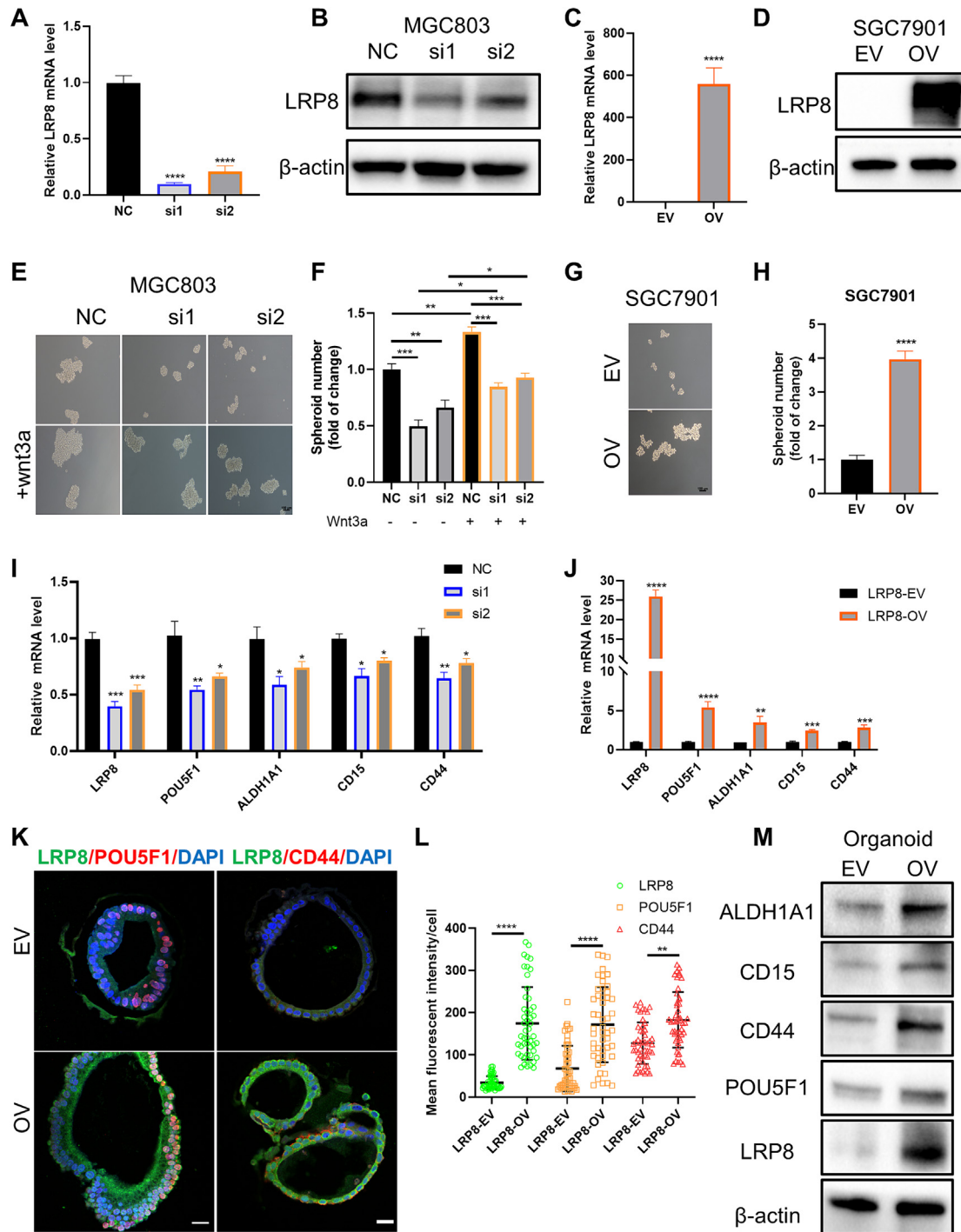


**Fig. 3. LRP8 promotes stemness of GC cells and organoids A-B.** The knockdown efficiency of LRP8 in MGC803 cells was identified by RT-qPCR(A) and western blot (B) methods. C-D. The LRP8 overexpressed SGC7901 cell line (LRP8-OV) and control expression vector cells (LRP8-EV) were established by lentiviral infection. The expression of LRP8 was identified by RT-qPCR and western blot method. E. Sphere formation efficiency of MGC803 cells with siLRP8 and cultured in stem cell medium for 7 days was determined. For rescue experiments, 20 % of Wnt3a medium was added. F. The numbers of MGC803 spheroids with a diameter > 100  $\mu$ m were counted (n = 3 independent experiments). G. Sphere formation was measured H. The numbers of SGC7901 spheroids with a diameter > 100  $\mu$ m were counted (n = 3 independent experiments). I. RT-qPCR was used to detect the expression of stemness-related genes (*POU5F1*, *ALDH1A1*, *CD15*, and *CD44*) in MGC803 spheroids transfected with siRNA targeting LRP8 (si1 and si2) or negative control (NC) and cultured with stem cell medium (n = 3 independent experiments). J. SGC7901 cells were infected with lentivirus generated by LRP8 empty vector (LRP8-EV) or LRP8 overexpressed vector (LRP8-OV) and cultured in stem cell medium for 3 days, and then the expression of stemness-related genes was detected (n = 3 independent experiments). K. Immunofluorescence detection of LRP8 (green) and POU5F1 (red on left) or CD44 (red on right) expression in LRP8-OV or LRP8-EV GC organoids, with a scale bar 20  $\mu$ m. L. The mean fluorescence intensity of 50 organoid cells is shown in the scatter plot. M. Western blot analysis of stem cell markers of LRP8-OV gastric cancer organoid (\*:  $p < 0.05$ , \*\*:  $p < 0.01$ , \*\*\*:  $p < 0.001$ , \*\*\*\*:  $p < 0.0001$ ). (For interpretation of the references to color in this figure legend, the reader is referred to the web version of this article.)

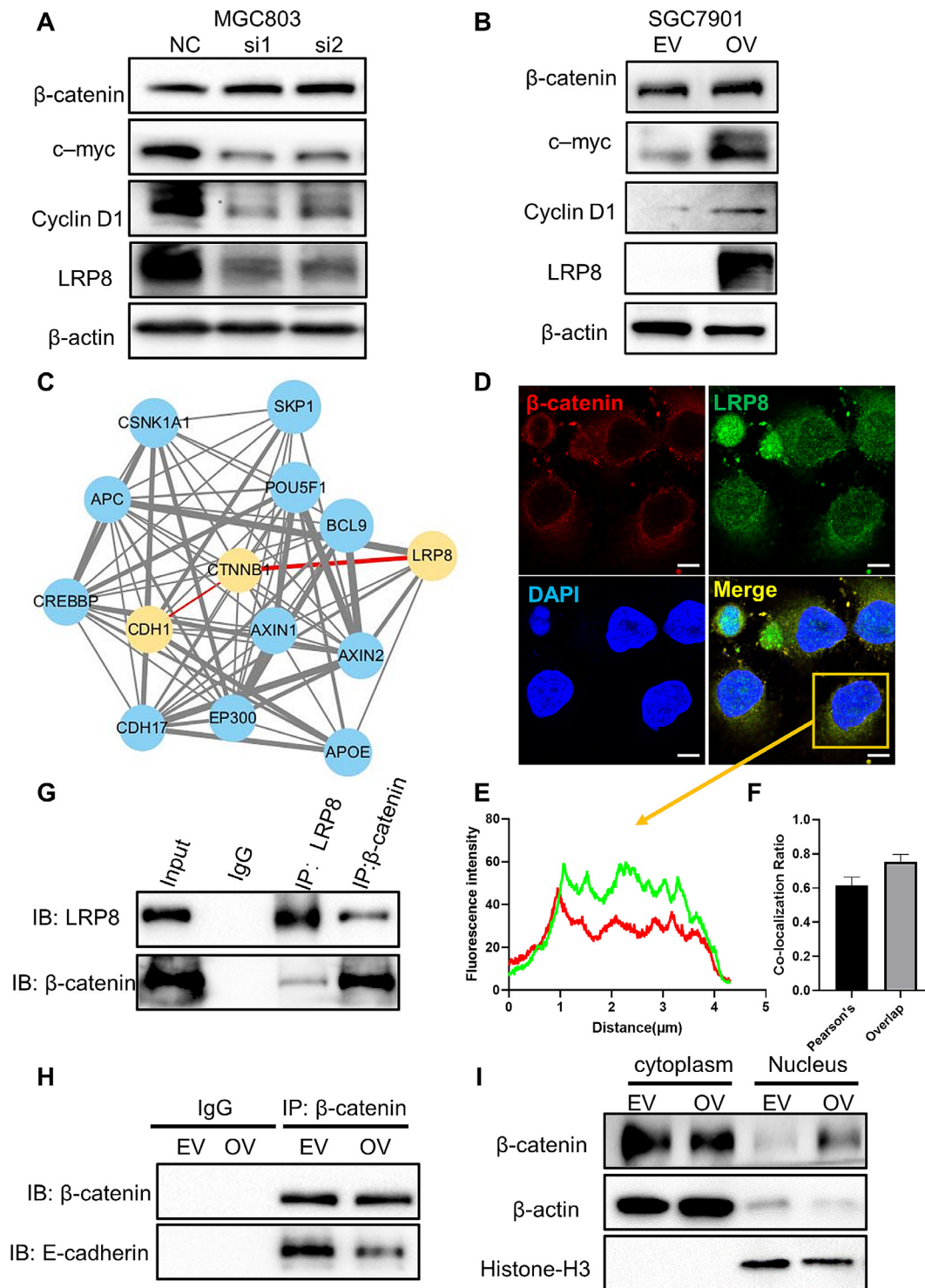


**Fig. 4. LRP8 interacts with β-catenin to regulate Wnt/β-catenin pathway activation.** **A.** β-catenin, c-myc, cyclin D1 and LRP8 protein expression in MGC803 cells transfected with si-LRP8 or negative control (NC) for 48 h were analyzed by Western blotting. **B.** cyclin D1, and c-myc protein expression in LRP8-overexpressing (OV) and EV SGC7901 cells (left panel) were analyzed by Western blotting. **C.** Protein-protein interaction networks between LRP8 and Wnt pathway proteins were generated from the STRING database. **D.** Immunofluorescence staining of LRP8 (red) and β-catenin (green) in SGC7901 cells, with DAPI (blue) indicating nuclei. Scale bar, 5 μm. **E-F.** Co-localization analysis of LRP8 and β-catenin using Pearson's correlation and overlap coefficient, with results presented in a bar graph format. **G.** Co-immunoprecipitation (Co-IP) assay demonstrated an interaction between LRP8 and β-catenin in LRP8-OV SGC7901 cells (IB, immunoblot). **H.** Co-IP assay was performed to measure the levels of E-cadherin/β-catenin complex in LRP8-EV and LRP8-OV cells. **I.** Western blot analysis of the intracellular distribution of LRP8 and β-catenin in the nuclear and cytoplasmic fractions of LRP8-EV and LRP8-OV SGC7901 cells. Histone-H3 and β-actin were used as internal controls for the nuclear and cytoplasmic proteins, respectively. (For interpretation of the references to color in this figure legend, the reader is referred to the web version of this article.)

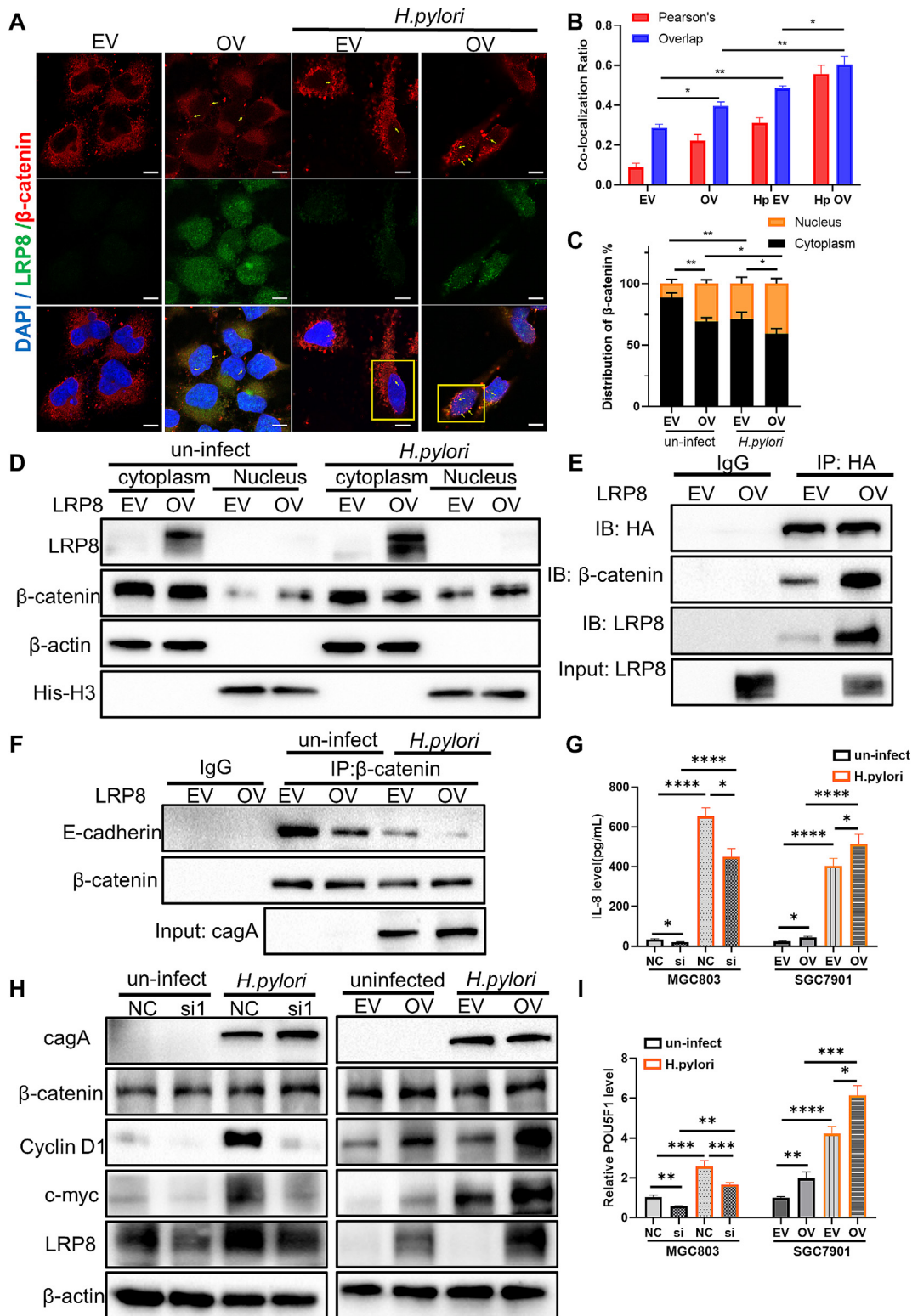


**Fig. 5.** *H. pylori* infection induced  $\beta$ -catenin transcriptional activity in a LRP8-dependent manner. **A.** Immunofluorescence staining of  $\beta$ -catenin in LRP8-EV and LRP8-OV SGC7901 cells infected with *H. pylori* P12 for 18 h, showing the intracellular distribution of  $\beta$ -catenin, white arrow points to the  $\beta$ -catenin foci in the nucleus. The scale bar represents 5  $\mu$ m. **B.** Semi-quantitative analysis of  $\beta$ -catenin nuclear localization using Pearson's correlation and the overlap coefficient, presented as bar graphs. **C-D.** Western blot analysis of the intracellular distribution of LRP8 and  $\beta$ -catenin in the nuclear and cytoplasmic fractions of LRP8-EV and LRP8-OV SGC7901 cells after an 18-hour infection with *H. pylori* P12 strain. Grayscale values of the bands in Figure D were obtained using Image J software. **E.** Co-immunoprecipitation (Co-IP) was performed to measure the levels of LRP8 and  $\beta$ -catenin in pcDNA3.1-HA-CagA plasmid transfected LRP8-EV and LRP8-OV SGC7901 cells. Proteins were collected and co-incubated with HA antibody-conjugated magnetic beads. **F.** Co-IP assay was performed to measure the levels of E-cadherin/ $\beta$ -catenin complex in LRP8-EV and LRP8-OV cells after infection with *H. pylori* P12 strains for 18 h. **G.** ELISA measurement of IL-8 cytokine production in culture supernatants from LRP8 knockdown MGC803 and LRP8-OV SGC7901 cells infected with *H. pylori* for 18 h (n = 3 independent experiments). **H.** Western blot analysis of  $\beta$ -catenin, cyclin D1 and c-myc expression in protein lysates from LRP8 knockdown MGC803 (left) and LRP8-overexpressing (OV) SGC7901 cells (right) infected with *H. pylori* P12 strain for 18 h. **I.** RT-qPCR analysis of POU5F1 expression in *H. pylori*-infected MGC803 cells with LRP8 knockdown and LRP8-overexpressing SGC7901 cells for 18 h (n = 3 independent experiments). (\*:  $p < 0.05$ , \*\*:  $p < 0.01$ , \*\*\*:  $p < 0.001$ , \*\*\*\*:  $p < 0.0001$ ).

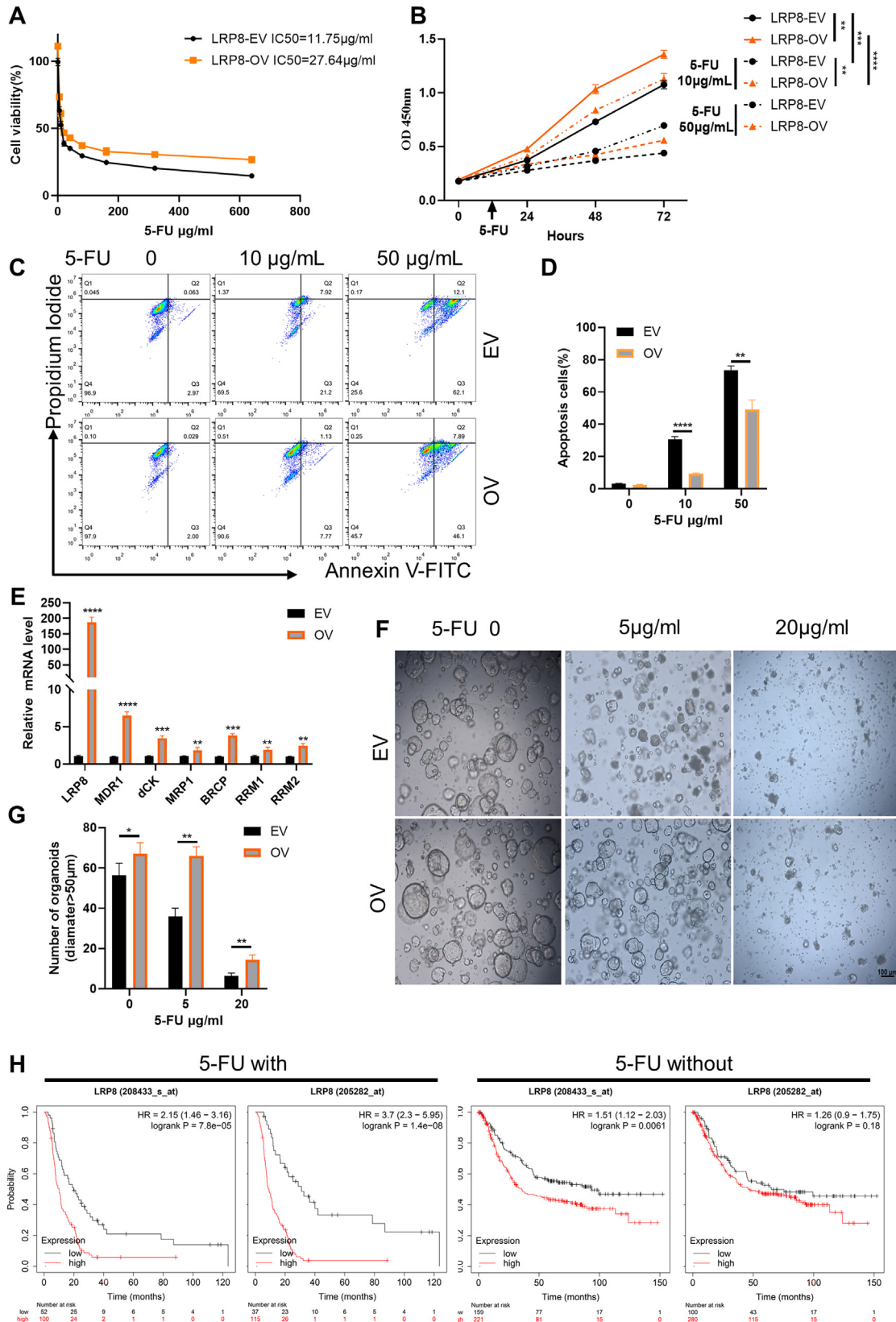


**Fig. 6.** LRP8 overexpression reduces the drug sensitivity of gastric cancer cells to 5-FU *in vitro*. **A.** Cell viability was measured using the CCK8 method in LRP8-EV and OV SGC7901 cells treated with different concentrations of 5-Fluorouracil (5-FU) for 48 h. The half inhibition concentrations (IC50) values were calculated using GraphPad software. **B.** Proliferation curves were plotted for LRP8-EV and OV SGC7901 cells treated with different concentrations of 5-FU (0, 10 and 50 µg/mL). **C.** Flow cytometry assay was performed to detect apoptotic cells in LRP8-EV and OV cells treated with 5-FU at different concentrations (0, 10 and 50 µg/mL). **D.** The proportion of apoptotic cells was quantified (n = 3). **E.** RT-qPCR was used to determine the expression levels of multidrug resistance (MDR) genes (*MDR-1*, *DCK*, *MRP1*, *BRCP*, *RRM1*, and *RRM2*) in LRP-EV and OV cells (n = 3). **F.** Representative micrographs of LRP8 EV and OV gastric cancer organoids treated with different concentrations of 5-FU. **G.** Number of organoids over 50 µm diameter. **H.** Kaplan-Meier survival curves were generated for gastric cancer patients in different LRP8 expression groups after 5-FU treatment. (\*: p < 0.05, \*\*: p < 0.01, \*\*\*: p < 0.001, \*\*\*\*: p < 0.0001).

traditional 2D cultures, we evaluated the impact of LRP8 on 5-FU sensitivity in organoids generated from tissues obtained from variety of clinical cases. LRP8 overexpressing in hGCO demonstrated increased size and number, indicating a resistance to 5-FU-induced cytotoxicity, compared with the control group (Fig. 6F, G).

A subgroup survival analysis highlighted the clinical implications of LRP8 expression levels in GC patients undergoing 5-FU-based chemotherapy (Fig. 6H). Patients with higher expression of LRP8 exhibited significantly shorter median survival times (9.2 months) compared to those with lower expression levels (31 months), underscoring the prognostic value of LRP8 in predicting chemotherapy outcomes (Table S4). These findings collectively point the critical role of LRP8 in modulating 5-FU chemosensitivity in GC, suggesting its utility as both a biomarker for chemotherapy response and a potential therapeutic target to overcome drug resistance.

## Discussion

We explored the complex molecular pathways involved in *H. pylori* infection-induced gastric carcinogenesis. We found that LRP8, which is upregulated in response to *H. pylori* infection both in laboratory cell cultures and mice, plays a crucial role in promoting stemness in GC cells and organoids by enhancing the transcriptional activity of  $\beta$ -catenin. LRP8 can be identified as an oncogene induced by *H. pylori* infection. This groundbreaking study establishes a novel connection between *H. pylori* infection and the initiation and progression of GC.

*H. pylori* is recognized as a class I carcinogen and is the primary risk factor for intestinal-type GC [29]. In our study, we identified an upregulation of LRP8 in gastric tissues infected with *H. pylori*, particularly pronounced in cases of intestinal-type GC. This finding hints at a potential link between LRP8 expression and GC progression. *H. pylori* infection induces several tissue changes, including inflammation, DNA damage, abnormal cell proliferation, and the activation of stem cell-like traits through the Wnt/ $\beta$ -catenin signaling pathway, all of which are pivotal in advancing GC [9,10,30–34]. CagA, is known to disrupt the E-cadherin/ $\beta$ -catenin complex, thereby activating the Wnt/ $\beta$ -catenin pathway in AGS cells [7]. However, in this study did not observe a direct interaction between CagA and E-cadherin *in vitro*, suggesting the possibility of CagA engage with other cellular components; thus we uncovered the formation of CagA/LRP8/ $\beta$ -catenin complexes. This suggests that LRP8, found both on the cell membrane and intracellularly, serves as an “anchor” that enables the initial interaction between CagA and  $\beta$ -catenin, promoting  $\beta$ -catenin’s nuclear translocation in GC cells. We observed that high LRP8 expression markedly enhances nuclear localization of  $\beta$ -catenin. In short, LRP8 upregulation facilitates increased nuclear translocation of  $\beta$ -catenin, leading to enhanced transcription of target genes.

LRP8, a key component of the LDL receptor family, plays a complex role in cancer, with its involvement in tumor progression and response to treatment varying across different cell types [35–38], while previous studies have highlighted the upregulation of LRP8 by miR142 and mycophenolic acid in GC cells [39,40]. In the current study we introduce a novel regulator of LRP8— $\beta$ -ADP-heptose, a virulence factor of *H. pylori*, distinct from the well-known CagA. We propose a model wherein  $\beta$ -ADP-heptose, produced at the onset of *H. pylori* infection, leads to LRP8 upregulation. This upregulation facilitates nuclear translocation of  $\beta$ -catenin either directly by LRP8 or indirectly by serving as a molecular bridge that strengthens the interaction between CagA and  $\beta$ -catenin. Consequently, this creates a positive feedback loop that amplifies the virulence effects of *H. pylori*, significantly boosting its transcriptional influence on the target genes of

Wnt/ $\beta$ -catenin pathway. Intriguingly, high expression of LRP8 might continue to increase  $\beta$ -catenin transcription even after eradicating *H. pylori* infection, offering a possible explanation for the progression to GC in some patients despite successful *H. pylori* eradication therapy [41]. This model highlights the intricate relationship between *H. pylori* infection, LRP8 expression, and  $\beta$ -catenin signaling in GC pathogenesis, pointing to LRP8 as a critical factor in the cancer development.

Our study delves into the implications of LRP8 expression for the treatment and prognosis of patients with gastric cancer, uncovering that those with LRP8-overexpressing GC tumors have diminished long-term survival rate, particularly noticeable in patients undergoing 5-FU chemotherapy. The challenge of chemoresistance is a significant barrier to effective patient care, often attributed to the presence of cancer cells with stem-like properties that are inherently resistant to treatment, enabling their survival and proliferation [42–46]; The role of *H. pylori* infection and consequent inflammation in promoting stem-like characteristics in cancer cells has been a focus of various models explaining this phenomenon. Given the heterogeneity of GC, employing robust *in-vitro* models to study the properties of CSC is critical [47]. Recent progress in this area includes the use of tumor spheroids [48] and gastric organoids [20], which are enriched with epithelial stem cells. These models serve as effective tools for pathogenesis studies and drug screening, accurately replicating the tumor microenvironment and facilitating the development of personalized treatment strategies [49,50].

Our findings reveal that LRP8 overexpression in GC cells leads to enhanced cell proliferation, increased sphere size and formation efficiency in GC organoids, and elevated expression of stemness markers in both GC spheroids and organoids. Moreover, we discovered that LRP8 overexpression significantly reduces 5-FU-induced apoptosis and decreases the sensitivity of hGCO to 5-FU, highlighting the role of LRP8 in promoting 5-FU resistance in GC cells. This is corroborated by organoid RNA-seq studies that identify LRP8 upregulation in 5-FU-resistant hGCO [51]. The impact of LRP8 on chemoresistance has also been observed in other cancer cell lines, including Huh7 and H460[18,52].

Taking into account the crucial role of LRP8 in cellular proliferation and its influence on cancer cell resistance to treatment, targeting LRP8 could present novel therapeutic opportunities to overcome GC. This approach has the potential to improve the efficacy of existing treatments and improve patient outcomes by addressing the root causes of chemoresistance.

## Conclusion

This study uncovers the bridging role of LRP8 in mediating the synergistic action between  $\beta$ -ADP-heptose derived from *H. pylori* and CagA, thus amplifying their virulence effects. Events involving LRP8 not only provide insights into the complex molecular mechanisms underlying GC pathogenesis but also highlight its potential role as a therapeutic target in *H. pylori* infection and GC development. These findings offer valuable implications for potential therapeutic strategies for combating *H. pylori*-associated gastric carcinogenesis.

## Credit author statement

**Liu Bin:** Conceptualization, Formal analysis, Investigation, Methodology, Writing first draft. **Ihtisham Bukhari:** Conceptualization, Formal Analysis, Methodology, Validation, Writing, Reviewing and editing Manuscript. **Fazhan Li:** Bioinformatics analysis, Formal analysis, Reviewing Manuscript. **Feifei Ren:** Methodology, Formal analysis. **Xue Xia:** Formal analysis, Review and

Editing manuscript. **Baitong Hu:** Methodology, Samples collection. **Haipeng Liu:** Conceptualization and Study design. **Thomas F Meyer:** Resources and Study design, Reviewing Manuscript. **Barry J Marshal:** Resources, Study design, Reviewing data. **Alfred Tay:** Resources, Methodology, Reviewing manuscript. **Yuming Fu:** Resources and Reviewing manuscript. **Youcai Tang:** Validation, Methodology and Reviewing manuscript. **Yang Mi:** Conceptualization, Supervision, Writing and Reviewing manuscript, Resources. **Peng-Yuan Zheng:** Conceptualization, Supervision, Project administration, Funding acquisition, Writing and Reviewing manuscript.

## Compliance with ethics requirements

All procedures followed were in accordance with the ethical standards of the responsible committee on human experimentation (institutional and national) and with the Helsinki Declaration of 1964, as revised in 2008 (5). Informed consent was obtained from all patients for being included in the study.

## Declaration of competing interest

The authors declare that they have no known competing financial interests or personal relationships that could have appeared to influence the work reported in this paper.

## Acknowledgements

We greatly thank the patients and their families for participating in our study. We are also highly grateful to the doctors, nurses, and paramedical staff of the Fifth affiliated hospital of Zhengzhou University for providing the samples. This work was funded by National Key Research and Development Program of China (No:2020YFC2006100), Zhengzhou Major Collaborative Innovation Project (No: 18XTZX12003) and Key Projects of Discipline Construction in Zhengzhou University (No: XKZDJC202001).

## Appendix A. Supplementary material

Supplementary data to this article can be found online at <https://doi.org/10.1016/j.jare.2024.04.002>.

## References

- Lin Y, Zheng Y, Wang HL, Wu J. Global patterns and trends in gastric cancer incidence rates (1988–2012) and predictions to 2030. *Gastroenterology* 2021;161(1):116–127.e8. doi: <https://doi.org/10.1053/j.gastro.2021.03.023>.
- Yan L, Chen Y, Chen F, Tao T, Hu Z, Wang J, et al. Effect of *Helicobacter pylori* Eradication on Gastric Cancer Prevention: Updated Report From a Randomized Controlled Trial With 26.5 Years of Follow-up. *Gastroenterology*. 163(1)(2022). 154–162.e3. <https://doi.org/10.1053/j.gastro.2022.03.039>.
- Wang F, Meng W, Wang B, Qiao L. *Helicobacter pylori*-induced gastric inflammation and gastric cancer. *Cancer Lett* 2014;345(2):196–202. doi: <https://doi.org/10.1016/j.canlet.2013.08.016>.
- Parsons MJ, Tammela T, Dow LE. WNT as a driver and dependency in cancer. *Cancer Discov* 2021;11(10):2413–29. doi: <https://doi.org/10.1158/2159-8290.CD-21-0190>.
- Katoh M, Katoh M. WNT signaling pathway and stem cell signaling network. *Clin Cancer Res* 2007;13(14):4042–5. doi: <https://doi.org/10.1158/1078-0432.CCR-06-2316>.
- Malfertheiner P, Camargo MC, El-Omar E, Liou JM, Peek R, Schulz C, et al. *Helicobacter pylori* infection. *Nature reviews Disease primers*. 9(1)(2023). 19. doi: 10.1038/s41572-023-00431-8.
- Murata-Kamiya N, Kurashima Y, Teishikata Y, Yamahashi Y, Saito Y, Higashi H, et al. *Helicobacter pylori* CagA interacts with E-cadherin and deregulates the beta-catenin signal that promotes intestinal transdifferentiation in gastric epithelial cells. *Oncogene* 2007;26(32):4617–26. doi: <https://doi.org/10.1038/sj.onc.1210251>.
- Sokolova O, Bozko PM, Naumann M. *Helicobacter pylori* suppresses glycogen synthase kinase 3beta to promote beta-catenin activity. *J Biol Chem* 2008;283(43):29367–74. doi: <https://doi.org/10.1074/jbc.M801818200>.
- Pfannkuch L, Hurwitz R, Traulsen J, Sigulla J, Poeschke M, Matzner L, et al. ADP heptose, a novel pathogen-associated molecular pattern identified in *Helicobacter pylori*. *FASEB J* 2019;33(8):9087–99. doi: <https://doi.org/10.1096/fi.201802555R>.
- Bauer M, Nascakova Z, Mihai AI, Cheng PF, Levesque MP, Lampart S, et al. The ALPK1/TIFA/NF- $\kappa$ B axis links a bacterial carcinogen to R-loop-induced replication stress. *Nature communications*. 11(1)(2020). 5117. doi: 10.1038/s41467-020-18857-z.
- Amieva M, Peek Jr RM. Pathobiology of *Helicobacter pylori*-induced gastric cancer. *Gastroenterology* 2016;150(1):64–78. doi: <https://doi.org/10.1053/j.gastro.2015.09.004>.
- Miyazawa K, Iwaya K, Kuroda M, Harada M, Serizawa H, Koyanagi Y, et al. Nuclear accumulation of beta-catenin in intestinal-type gastric carcinoma: correlation with early tumor invasion. *Virchows Arch* 2000;437(5):508–13. doi: <https://doi.org/10.1007/s004280000283>.
- Passarella D, Ciampi S, Di Liberto V, Zuccarini M, Ronci M, Medoro A, et al. Low-Density Lipoprotein Receptor-Related Protein 8 at the Crossroad between Cancer and Neurodegeneration. *Int J Mol Sci*. 23(16)(2022). <https://doi.org/10.3390/ijms23168921>.
- Go GW, Mani A. Low-density lipoprotein receptor (LDLR) family orchestrates cholesterol homeostasis. *Yale J Biol Med*. 85(1)(2012). 19–28. doi: 10.1007/s12072-012-9161-1.
- Zhang J, Zhang X, Zhou F, van Dinther M, Ten Dijke P. LRP8 mediates wnt/ $\beta$ -catenin signaling and controls osteoblast differentiation. *J Bone Miner Res* 2012;27(10):2065–74. doi: <https://doi.org/10.1002/jbmr.1661>.
- Pencheva N, Tran H, Buss C, Huh D, Drobnjak M, Busam K, et al. Convergent multi-miRNA targeting of ApoE drives LRP1/LRP8-dependent melanoma metastasis and angiogenesis. *Cell* 2012;151(5):1068–82. doi: <https://doi.org/10.1016/j.cell.2012.10.028>.
- Li C, Yang Y, Wang H, Song Y, Huang H. miR-362-3p suppresses ovarian cancer by inhibiting LRP8. *Transl Oncol*. 15(1)(2022). 101284. <https://doi.org/10.1016/j.tranon.2021.101284>.
- Fang Z, Zhong M, Zhou L, Le Y, Wang H, Fang Z. Low-density lipoprotein receptor-related protein 8 facilitates the proliferation and invasion of non-small cell lung cancer cells by regulating the wnt/ $\beta$ -catenin signaling pathway. *Bioengineered* 2022;13(3):6807–18. doi: <https://doi.org/10.1080/21655979.2022.2036917>.
- Lin CC, Lo MC, Moody R, Jiang H, Harouaka R, Stevers N, et al. Targeting LRP8 inhibits breast cancer stem cells in triple-negative breast cancer. *Cancer Lett* 2018;438:165–73. doi: <https://doi.org/10.1016/j.canlet.2018.09.022>.
- Schlaermann P, Toelle B, Berger H, Schmidt SC, Glanemann M, Ordemann J, et al. A novel human gastric primary cell culture system for modelling *Helicobacter pylori* infection in vitro. *Gut* 2016;65(2):202–13. doi: <https://doi.org/10.1136/gutjnl-2014-307949>.
- Lee A, O'Rourke J, De Ungria MC, Robertson B, Daskalopoulos G, Dixon MF. A standardized mouse model of *Helicobacter pylori* infection: introducing the Sydney strain. *Gastroenterology* 1997;112(4):1386–97. doi: [https://doi.org/10.1016/s0016-5085\(97\)70155-0](https://doi.org/10.1016/s0016-5085(97)70155-0).
- Li H, Tang H, Debowski AW, Stubbs KA, Marshall BJ, Benghezal M. Lipopolysaccharide Structural Differences between Western and Asian *Helicobacter pylori* Strains. *Toxins (Basel)*. 10(9)(2018). <https://doi.org/10.3390/toxins10090364>.
- Liu B, Liu HP, Ren FF, Liu HF, Bukhari I, Fu YM, et al. cGAS regulates the DNA damage response to maintain proliferative signaling in gastric cancer cells. *Oncol Res* 2022;29(2):87–103. doi: <https://doi.org/10.32604/or.2022.03529>.
- Sun L, Huang C, Zhu M, Guo S, Gao Q, Wang Q, et al. Gastric cancer mesenchymal stem cells regulate PD-L1-CTCF enhancing cancer stem cell-like properties and tumorigenesis. *Theranostics* 2020;10(26):11950–62. doi: <https://doi.org/10.7150/thno.49717>.
- Bustin SA, Benes V, Garson JA, Hellemans J, Huggett J, Kubista M, et al. The MIQE guidelines: minimum information for publication of quantitative real-time PCR experiments. *Clin Chem* 2009;55(4):611–22. doi: <https://doi.org/10.1373/clinchem.2008.112797>.
- O'Brien CE, Bonanno L, Zhang H, Wyss-Coray T. Beclin 1 regulates neuronal transforming growth factor- $\beta$  signaling by mediating recycling of the type I receptor ALK5. *Mol Neurodegener*. 10(2015). 69. <https://doi.org/10.1186/s13024-015-0065-0>.
- McGough IJ, Steinberg F, Jia D, Barbuti PA, McMillan KJ, Heesom KJ, et al. Retromer binding to FAM21 and the WASH complex is perturbed by the Parkinson disease-linked VPS35(D620N) mutation. *Curr Biol* 2014;24(14):1670–6. doi: <https://doi.org/10.1016/j.cub.2014.06.024>.
- Vasan N, Baselga J, Hyman DM. A view on drug resistance in cancer. *Nature* 2019;575(7782):299–309. doi: <https://doi.org/10.1038/s41586-019-1730-1>.
- Gobert AP, Wilson KT. Induction and regulation of the innate immune response in *Helicobacter pylori* infection. *Cell Mol Gastroenterol Hepatol* 2022;13(5):1347–63. doi: <https://doi.org/10.1016/j.cjcmgh.2022.01.022>.
- Abdi E, Latifi-Navid S, Abedi Sarvestani F, Esmailnejad MH. Emerging therapeutic targets for gastric cancer from a host-*Helicobacter pylori* interaction perspective. *Expert Opin Ther Targets* 2021;25(8):685–99. doi: <https://doi.org/10.1080/14728222.2021.1971195>.

- [31] Novak A, Dedhar S. Signaling through beta-catenin and Lef/Tcf. *Cell Mol Life Sci* 1999;56(5–6):523–37. doi: <https://doi.org/10.1007/s000180050449>.
- [32] Zhan T, Rindtorff N, Boutros M. Wnt signaling in cancer. *Oncogene* 2017;36(11):1461–73. doi: <https://doi.org/10.1038/onc.2016.304>.
- [33] Seeneevassen L, Bessède E, Mégraud F, Lehours P, Dubus P, Varon C. Gastric cancer: advances in Carcinogenesis Research and new therapeutic strategies. *Int J Mol Sci* 2021;22(7). doi: <https://doi.org/10.3390/ijms22073418>.
- [34] Bessède E, Staedel C, Acuña Amador LA, Nguyen PH, Chambonnier L, Hatakeyama M, et al. Helicobacter pylori generates cells with cancer stem cell properties via epithelial-mesenchymal transition-like changes. *Oncogene* 2014;33(32):4123–31. doi: <https://doi.org/10.1038/onc.2013.380>.
- [35] Tavazoie MF, Pollack I, Tanqueco R, Ostendorf BN, Reis BS, Gonsalves FC, et al. LXR/ApoE activation restricts innate immune suppression in cancer. *Cell* 2018;172(4):825–840.e18. doi: <https://doi.org/10.1016/j.cell.2017.12.026>.
- [36] Li L, Qu WH, Ma HP, Wang LL, Zhang YB, Ma Y. LRP8, modulated by miR-1262, promotes tumour progression and forecasts the prognosis of patients in breast cancer. *Arch Physiol Biochem* 2022;128(3):657–65. doi: <https://doi.org/10.1080/13813455.2020.1716019>.
- [37] Li Z, Ferguson L, Deol KK, Roberts MA, Magtanong L, Hendricks JM, et al. Ribosome stalling during selenoprotein translation exposes a ferroptosis vulnerability. *Nat Chem Biol* 2022;18(7):751–61. doi: <https://doi.org/10.1038/s41589-022-01033-3>.
- [38] Alborzina H, Chen Z, Yildiz U, Freitas FP, Vogel FCE, Varga JP, et al. LRP8-mediated selenocysteine uptake is a targetable vulnerability in MYCN-amplified neuroblastoma. *EMBO Mol Med* 2023;15(8):e18014.
- [39] Lu J, Ma Y, Zhao Z. MiR-142 suppresses progression of gastric carcinoma via directly targeting LRP8. *Clin Res Hepatol Gastroenterol* 2021;45(4):. doi: <https://doi.org/10.1016/j.clinre.2020.08.001>101520.
- [40] Dun B, Sharma A, Teng Y, Liu H, Purohit S, Xu H, et al. Mycophenolic acid inhibits migration and invasion of gastric cancer cells via multiple molecular pathways. *PLoS One* 2013;8(11):e81702.
- [41] Collatuzzo G, Pelucchi C, Negri E, López-Carrillo L, Tsugane S, Hidaka A, et al. Exploring the interactions between Helicobacter pylori (hp) infection and other risk factors of gastric cancer: a pooled analysis in the stomach cancer pooling (StoP) project. *Int J Cancer* 2021;149(6):1228–38. doi: <https://doi.org/10.1002/ijc.33678>.
- [42] Deng J, Miller SA, Wang HY, Xia W, Wen Y, Zhou BP, et al. beta-catenin interacts with and inhibits NF-kappa B in human colon and breast cancer. *Cancer Cell* 2002;2(4):323–34. doi: [https://doi.org/10.1016/s1535-6108\(02\)00154-x](https://doi.org/10.1016/s1535-6108(02)00154-x).
- [43] Gambhir S, Vyas D, Hollis M, Aekka A, Vyas A. Nuclear factor kappa B role in inflammation associated gastrointestinal malignancies. *World J Gastroenterol* 2015;21(11):3174–83. doi: <https://doi.org/10.3748/wjg.v21.i11.3174>.
- [44] Sokolova O, Naumann M. NF-κB signaling in gastric cancer. *Toxins (Basel)* 2017;9(4). doi: <https://doi.org/10.3390/toxins9040119>.
- [45] Kwon OH, Kim JH, Kim SY, Kim YS. TWEAK/Fn14 signaling mediates gastric cancer cell resistance to 5-fluorouracil via NF-κB activation. *Int J Oncol* 2014;44(2):583–90. doi: <https://doi.org/10.3892/ijco.2013.2211>.
- [46] Ghatak S, Hascall VC, Karamanos N, Markwald RR, Misra S. Chemotherapy induces feedback up-regulation of CD44v6 in colorectal cancer initiating cells through β-catenin/MDR1 signaling to sustain chemoresistance. *Front Oncol* 2022;12(2022). 906260. <https://doi.org/10.3389/fonc.2022.906260>.
- [47] Giannakis M, Chen SL, Karam SM, Engstrand L, Gordon JI. Helicobacter pylori evolution during progression from chronic atrophic gastritis to gastric cancer and its impact on gastric stem cells. *Proceedings of the National Academy of Sciences of the United States of America*. 105(11)(2008). 4358–63. <https://doi.org/10.1073/pnas.0800668105>.
- [48] Gunti S, Hoke ATK, Vu KP, London Jr NR. Organoid and spheroid tumor models: techniques and applications. *Cancers (Basel)* 2021;13(4). doi: <https://doi.org/10.3390/cancers13040874>.
- [49] Yan HHN, Siu HC, Law S, Ho SL, Yue SSK, Tsui WY, et al. A comprehensive human gastric cancer organoid biobank captures tumor subtype heterogeneity and enables therapeutic screening. *Cell Stem Cell* 2018;23(6):882–897.e11. doi: <https://doi.org/10.1016/j.stem.2018.09.016>.
- [50] Steele NG, Chakrabarti J, Wang J, Biesiada J, Holokai L, Chang J, et al. An organoid-based preclinical model of human gastric cancer. *Cell Mol Gastroenterol Hepatol* 2019;7(1):161–84. doi: <https://doi.org/10.1016/j.jcmgh.2018.09.008>.
- [51] Ukai S, Honma R, Sakamoto N, Yamamoto Y, Pham QT, Harada K, et al. Molecular biological analysis of 5-FU-resistant gastric cancer organoids; KHDRBS3 contributes to the attainment of features of cancer stem cell. *Oncogene* 2020;39(50):7265–78. doi: <https://doi.org/10.1038/s41388-020-01492-9>.
- [52] Cai J, Chen J, Wu T, Cheng Z, Tian Y, Pu C, et al. Genome-scale CRISPR activation screening identifies a role of LRP8 in sorafenib resistance in Hepatocellular carcinoma. *Biochem Biophys Res Commun* 2020;526(4):1170–6. doi: <https://doi.org/10.1016/j.bbrc.2020.04.040>.